Optik 127 (2016) 5430–5438

Contents lists available at ScienceDirect

Optik

journal homepage: www.elsevier.de/ijleo

Original research article

An evolutionary approach for image retrieval based on lateral inhibition

Bai Li*

College of Control Science and Engineering, Zhejiang University, Hangzhou 310027, PR China

ARTICLE INFO

Article history:
Received 18 January 2016
Accepted 19 February 2016

Keywords:
Image retrieval
Lateral inhibition
Numerical optimization
Evolutionary algorithm
Artificial bee colony algorithm

ABSTRACT

Image retrieval refers to searching for specific pattern when browsing digital images in large databases. It is a fundamental topic in visual pattern recognition. The original image retrieval scheme is converted into a 2-dimensional optimization problem, during which image enhancement, a preprocessing step, is implemented to ease the template matching procedure. Image enhancement is achieved via lateral inhibition. Fundamental issues in this topic are investigated in this paper: (1) whether it is sensible to adopt an evolutionary algorithm to search for the best-match result, given that the concerned optimization problem has merely two dimensions; (2) how lateral inhibition takes effect to facilitate image retrieval. According to our comparative experimental results, there is no evidence that indicates lateral inhibition makes any subtle effort to ease the best-match optimization process. This paper also provides theoretical analyses regarding the evolutionary algorithm adopted.

1. Introduction

Image retrieval refers to the action of browsing and searching for digital images in large databases [1]. The incessant developments in image capturing devices and social media have led to an increase in the size of digital image collection, further aggravating the challenges to manual image retrieval in a variety of fields, including remote sensing [2–5], disease diagnosis [6–9], archive management [10,11], crime prevention [12,13], social networking service [14–16], etc. Numerous image retrieval methodologies have been developed and investigated, most of which have been broadly classified into two groups, namely, text-based and content-based methods: text-based methods are featured by the utilization of text descriptors to annotate images [17]; content-based methods aim to index images by their visual content (e.g., color, texture, shapes) [18]. This study focuses on content-based image retrieval.

How to search for a perfect match between a pre-define template and a candidate test image in the database is a critical issue in image retrieval. Given some specific similarity measurement criterion, evolutionary optimizers have been prevailing proposed to search for best-match solutions, e.g., chaotic quantum-behaved particle swarm optimization algorithm [19], Cauchy biogeography-based optimization algorithm [20], chaotic differential search algorithm [21], particle chemical reaction optimization algorithm [22], electimize approach [23] and imperialist competitive algorithm [24]. However, research studies in this community have been focusing overly on the computational efficiency of the optimizers, disregarding evaluating the entire approach in real-world problems [25,26]. As a remedy for the limitations in previous studies, this work provides in-depth analyses on the efficiency of evolutionary algorithms and the performance of lateral inhibition process to facilitate image retrieval.

The remainder of this paper is organized as follows. In Section 2, lateral inhibition based image retrieval model and our adopted optimizer are introduced. Simulations results are reported in Section 3, followed by detailed discussions in Section 4. Conclusions are drawn in Section 5.

2. Image retrieval scheme formulation

Image retrieval concerns about locating a given template image in a test image such that they best match each other. In this section, the image retrieval scheme is converted to a numerical optimization problem, during which an image enhancement process is implemented to ease the subsequent matching procedure.

2.1. Image matching principle and similarity measurement

Assuming that both the template image and the test image are described in gray-scale pixels, we describe the template image in a

* Tel.: +86 15700080810.
E-mail addresses: libaioutstanding@163.com, libai@zju.edu.cn

http://dx.doi.org/10.1016/j.ijleo.2016.02.056
0030-4026/

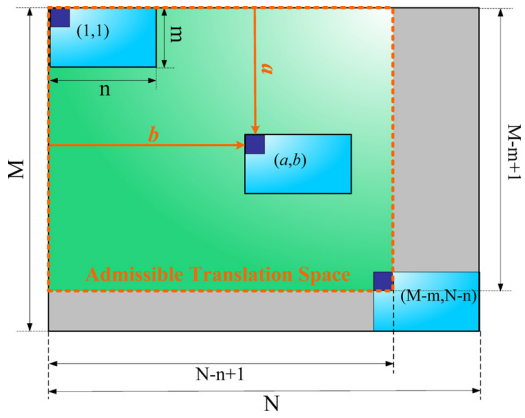

Fig. 1. Schematics on template translation. In this particular case, integer $a \in [1, M - m + 1]$, and integer $b \in [1, N - n + 1]$.

matrix form $\mathbf{temp}_{m\times n}$, wherein each element $\mathbf{temp}(\cdot,\cdot)$ records the gray level of the corresponding pixel location [5]. This induces that $\mathbf{temp} \in \mathbb{Z}^{m\times n} \cap [0, 255]^{m\times n}$. Similarly, the test image is described by matrix $\mathbf{test}_{M\times N} \in \mathbb{Z}^{M\times N} \cap [0, 255]^{M\times N}$. Now the original image retrieval problem becomes seeking for specific translations of $\mathbf{temp}_{m\times n}$ that maximize the similarity between **temp** and matrix

$$\begin{bmatrix} \mathbf{test}(a,b) & \cdots & \mathbf{test}(a,b+n-1) \\ \vdots & \ddots & \vdots \\ \mathbf{test}(a+m-1,b) & \cdots & \mathbf{test}(a+m-1,\ b+n-1) \end{bmatrix},$$

in which a denotes horizontal translation, and b denotes vertical translation of $\mathbf{temp}_{m\times n}$ (Fig. 1). The well-known normalized cross correlation (NCC) criterion [5] is adopted to measure the similarity according to the translation pair (a, b):

$$NCC(a,b) = \frac{\sum_{x=1}^{m}\sum_{y=1}^{n}[\mathbf{temp}(a+x-1,b+y-1)\cdot\mathbf{test}(x,y)]}{\sqrt{\sum_{x=1}^{m}\sum_{y=1}^{n}[\mathbf{temp}^2(a+x-1,b+y-1)]}\cdot\sqrt{\sum_{x=1}^{m}\sum_{y=1}^{n}[\mathbf{test}^2(x,y)]}}. \quad (1)$$

It is easy to see that $NCC(\cdot,\cdot) \in [0, 1]$, and the optimal translation pair (a^*, b^*) would render $NCC(a^*, b^*)=1$.

2.2. Image enhancement via lateral inhibition

Image enhancement is implemented to facilitate the subsequent image matching process. This subsection involves image enhancement via lateral inhibition.

Lateral inhibition principle was discovered by Hartline and Graham in a limulus vision experiment, and this concept was introduced for digital image processing later [27]. Specifically, in our adopted lateral inhibition model [19], an original gray-scale image is denoted as $\mathbf{I}_0$ and the enhanced one is denoted as $\mathbf{R}$. Lateral inhibition is implemented according to

$$\mathbf{R}(x,y) = \mathbf{I}_0(x,y) + \sum_{i=-A}^{A}\sum_{j=-B}^{B}\alpha_{ij}\cdot\mathbf{I}_0(x+i,y+j), \quad (2)$$

where $\mathbf{I}_0(x, y)$ refers to the original pixel gray level at (x, y), $\mathbf{R}(x, y)$ denotes the enhanced pixel gray level, α_{ij} is an inhibition weight parameter, A and B determine the inhibition scale. There are various ways to select α_{ij}, but the following requirement should be satisfied for balanced inhibition energy:

$$\sum_{i=-A}^{A}\sum_{j=-B}^{B}\alpha_{ij} = 0. \quad (3)$$

This present work adopts the definition of inhibition weight matrix in Ref. [27], wherein $[\alpha_{ij}]_{(2A+1)\times(2B+1)}$ is square and forms ρ rings (i.e., $A = B = \rho$). Specifically, each element α_r along the rth ring is defined as

$$\alpha_r = \begin{cases} 1 & \text{if } r = \rho \\ \dfrac{-1-r}{4(\rho+2)(\rho-1)(\rho-r)} & \text{if } r \le \rho - 1 \end{cases}. \quad (4)$$

Note that Eq. (3) holds true constantly according to the restrictions in Eq. (4). An instance under the condition that $\rho = 3$ is depicted in Fig. 2.

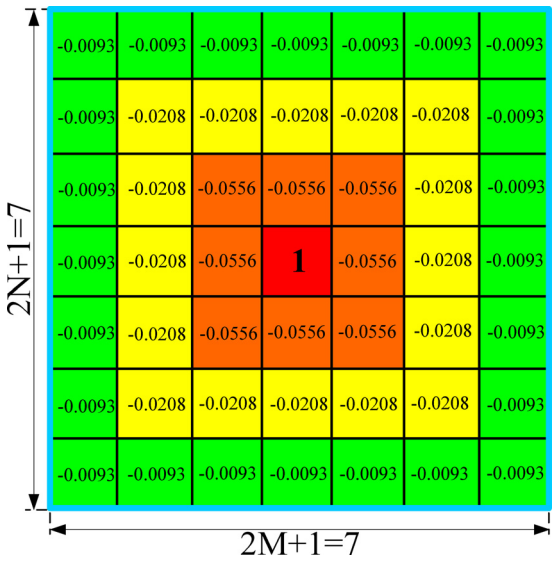

Fig. 2. Schematics on inhibition weight matrix based on the ring-like restrictions in Ref. [27] and $M = N = \rho = 3$.

2.3. Best-match location search via an evolutionary algorithm

This subsection is about how to find the very translation pair (a^*, b^*) that maximizes $NCC(\cdot, \cdot)$. An evolutionary algorithm, namely, artificial bee colony (ABC) algorithm, is adopted to seek for (a^*, b^*).

In ABC algorithm, the bee swarm mainly consists of two groups, namely employed bees and onlooker bees [5]. Employed bees are responsible for global exploration and onlooker bees for local exploitation. Some well-known studies alleged that ABC algorithm is good at global exploration but poor at local exploitation [28–30], but they failed to fully understand the local exploitation stage in ABC. In more detail, prevailing research studies believe that the local search intensity in the conventional ABC algorithm is not so delicate as to meet high-accuracy search demands (e.g., the self-adaptive ABC variants [31–39]). But those studies may have disregarded roulette selection, which plays a critical role in sorting qualified candidates (i.e. employed bees) in preparation of local exploitation. Suppose there is one employed bee that is significantly superior to all the rest candidates (regarding solution quality), it is very likely that all the onlooker bees would crossover & mutate around that employed bee, because the probability to follow any other employed bee is significantly smaller. Although not being delicate in crossover & mutation, yet local exploitation is enhanced via more trials. Thus to criticize the local search capability of ABC

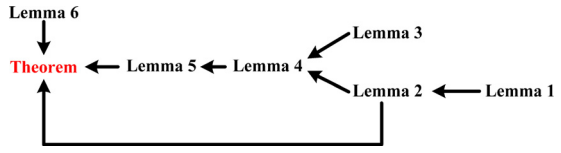

Fig. 3. Pathway of convergence analysis of ABC algorithm.

through intuition is not sensible. A recent study [40] even verified that several state-of-the-art ABC variants perform no better than the original ABC algorithm in an optimization problem that is similar to the one we concern. Through the aforementioned analyses, the author advocates that any new update to any conventional evolutionary algorithm should be verified by fair and solid comparative experiments [26], rather than by intuition or unjustifiable subjective knowledge.

Convergence analysis of ABC algorithm is given at the end of this subsection. An overview of the analytical procedure is shown in Fig. 3, where the establishment of **Theorem** is the ultimate goal. For convenience's sake, in-depth proofs are presented in **Appendix**.

Lemma 1 ((Borel–Lebesgue Theorem [41])). Let $\mathbf{A} \subseteq \mathbb{R}^w$ denote a bounded closed set and let $\mathbf{G}$ denote an open cover of $\mathbf{A}$. This assumption leads to a finite number of subsets $G_i \subseteq \mathbf{G}(i = 1, 2, \ldots, N_f)$ are then obtained, the union of which will be a cover of $\mathbf{A}$, i.e., $\mathbf{A} \subseteq \bigcup_{i=1}^{N_f} G_i$.

Lemma 2. When an objective function $fun(\bullet)$ is uniformly continuous in a continuous, closed, and bounded domain $\mathbf{D} \subseteq \mathbb{R}^w$, the infinite feasible solutions can be completely represented by a finite number of "elements".

The search for the global optimum can be considered a Markov process [42]. In that case, each underlying solution is an admissible state in the state vector $\mathbf{S} = \{\mathbf{S}_i | i = 1, 2, \ldots, N_{fs}\}$. A probability transition matrix $\mathbf{TP} \in \mathbb{R}^{N_{fs} \times N_{fs}}$ is then defined in Eq. (5), where tp_{ij} denotes the state transition probability from $\mathbf{S}_i$ to $\mathbf{S}_j$. According to Lemma 2, N_{fs} is a finite integer.

$$\mathrm{TP} = \begin{pmatrix} tp_{11} & \cdots & tp_{1N_{fs}} \\ tp_{21} & \cdots & tp_{2N_{fs}} \\ \vdots & \ddots & \vdots \\ tp_{N_{fs}1} & \cdots & tp_{N_{fs}N_{fs}} \end{pmatrix}_{N_{fs} \times N_{fs}} \tag{5}$$

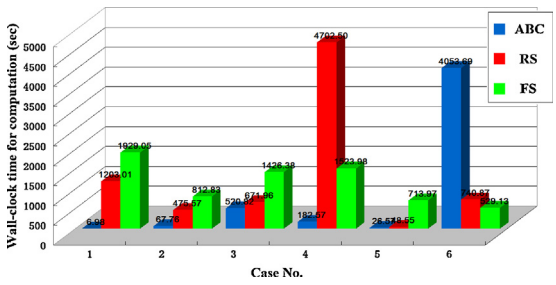

Fig. 5. Comparative average complete time for each of the three best-match searchers (i.e., ABC, RS, and FS) in each of the six cases.

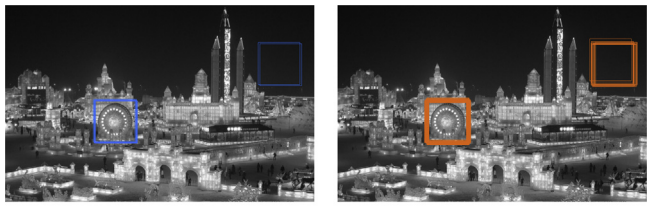

Fig. 6. Multiple optimization results within 6.98 s in Case 1: (a) using ABC, and (b) using RS.

Lemma 3. The current-best solution transition procedure in ABC algorithm is a stochastic process.

Lemma 4. The current-best solution transition process in ABC algorithm is a finite homogeneous Markov process.

Let $\mathbf{TP}_{t,t+1}$ denote the best-ever solution transition probability matrix from step t to step $t+1$. Entries in $\mathbf{TP}_{t+k,t+k+1}$ are denoted by tp_{ij}^k, $k \geq 0, i, j = 1, 2, \ldots, N_{fs}$.

Lemma 5.

$$\mathbf{TP}_{t,t+1} \cdot \mathbf{TP}_{t+1,t+2} = \mathbf{TP}_{t,t+2}.$$

Lemma 5 can be extended to a general form, where $T \in \mathbb{N}^*$

$$\mathbf{TP}_{1,T} = \prod_{i=1}^{T} \mathbf{TP}_{i,i+1}. \tag{6}$$

Eq. (6) and Lemma 4 yield

$$\mathbf{TP}_{1,T} = \prod_{i=1}^{T} \mathbf{TP}_{1,2}. \tag{7}$$

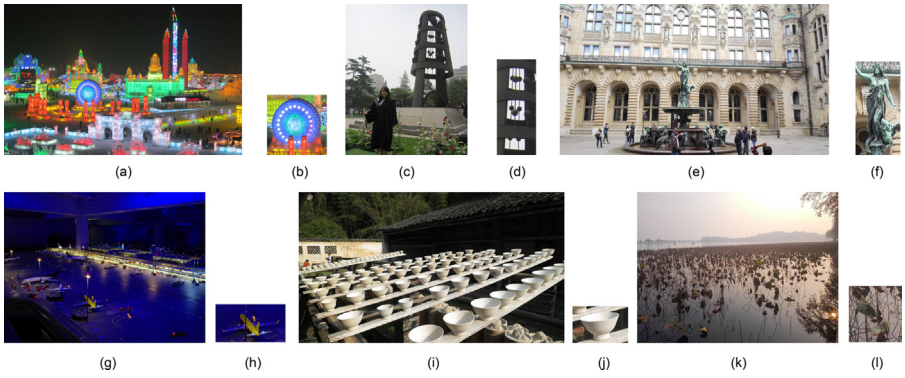

Fig. 4. Image retrieval scheme details: (a) test image in case 1 (Harbin Ice & Snow World); (b) template image in Case 1; (c) test image in case 2 (Beijing Normal University); (d) template image in Case 2; (e) test image in case 3 (Hamburg Rathaus); (f) template image in Case 3; (g) test image in case 4 (Hamburg Miniatur Wonderland); (h) template image in Case 4; (i) test image in case 5 (Jingdezhen Ceramic Museum); (j) template image in Case 5; (k) test image in case 6 (Hangzhou West Lake); and (l) template image in Case 6.

(a) (b)

Fig. 7. Multiple optimization results within 67.76 s in Case 2: (a) using ABC, and (b) using RS.

(a) (b)

Fig. 8. Multiple optimization results within 520.82 s in Case 3: (a) using ABC, and (b) using RS.

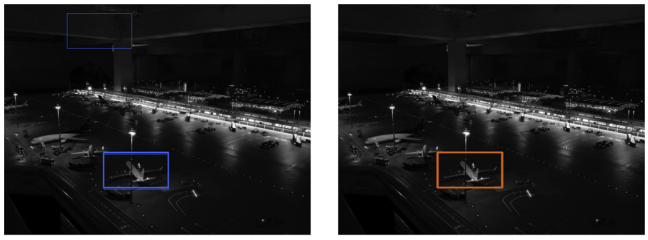

(a) (b)

Fig. 9. Multiple optimization results within 182.57 s in Case 4: (a) using ABC, and (b) using RS.

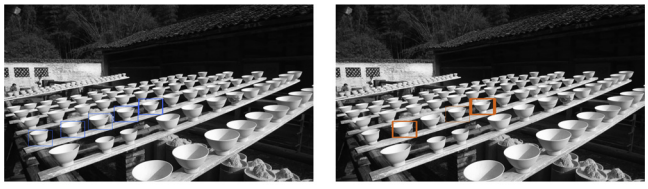

(a) (b)

Fig. 10. Multiple optimization results within 26.57 s in Case 5: (a) using ABC, and (b) using RS.

A square matrix **W** is reducible, if and only if **W** can be transformed into the following form (with square matrices **C** and **T**) [43].

$$W = \begin{pmatrix} \mathbf{C} & 0 \\ \mathbf{R} & \mathbf{T} \end{pmatrix} \tag{8}$$

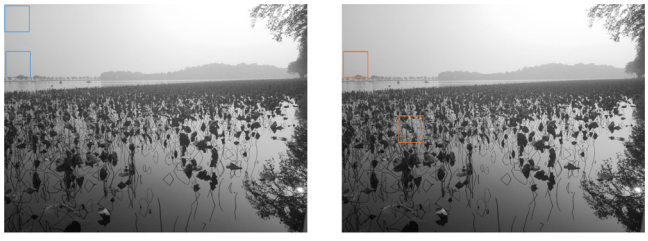

(a) (b)

Fig. 11. Multiple optimization results within 529.13 s in Case 6: (a) using ABC, and (b) using RS.

Lemma 6 ([44]). Let **W** be a reducible stochastic matrix in the form of Eq. (8). If **C** is a primitive stochastic matrix and **R**, **T** $\neq$ 0, then

$$\lim_{k\to\infty} \mathbf{W}^k = \lim_{k\to\infty} \begin{pmatrix} \mathbf{C}^k & 0 \\ \sum_{i=0}^{k-1} \mathbf{T}^i \mathbf{R} \mathbf{C}^{k-i} & \mathbf{T}^k \end{pmatrix} = \begin{pmatrix} \lim_{k\to\infty} \mathbf{C}^k & 0 \\ \mathbf{R}_\infty & 0 \end{pmatrix} \tag{9}$$

is a stable stochastic matrix.

Theorem. The transition of the current-best solution in ABC algorithm leads to the acquisition of the global minimum in the domain.

3. Simulations results

This section reports the simulation results. All the experiments were implemented in MATLAB R2015a and executed on an Intel Core i7-4710MQ CPU with 4 GB RAM that runs at 2.50 GHz under Microsoft Windows 7. The lateral inhibition weight matrix was defined in Fig. 2. User-specified parameters in ABC algorithm were

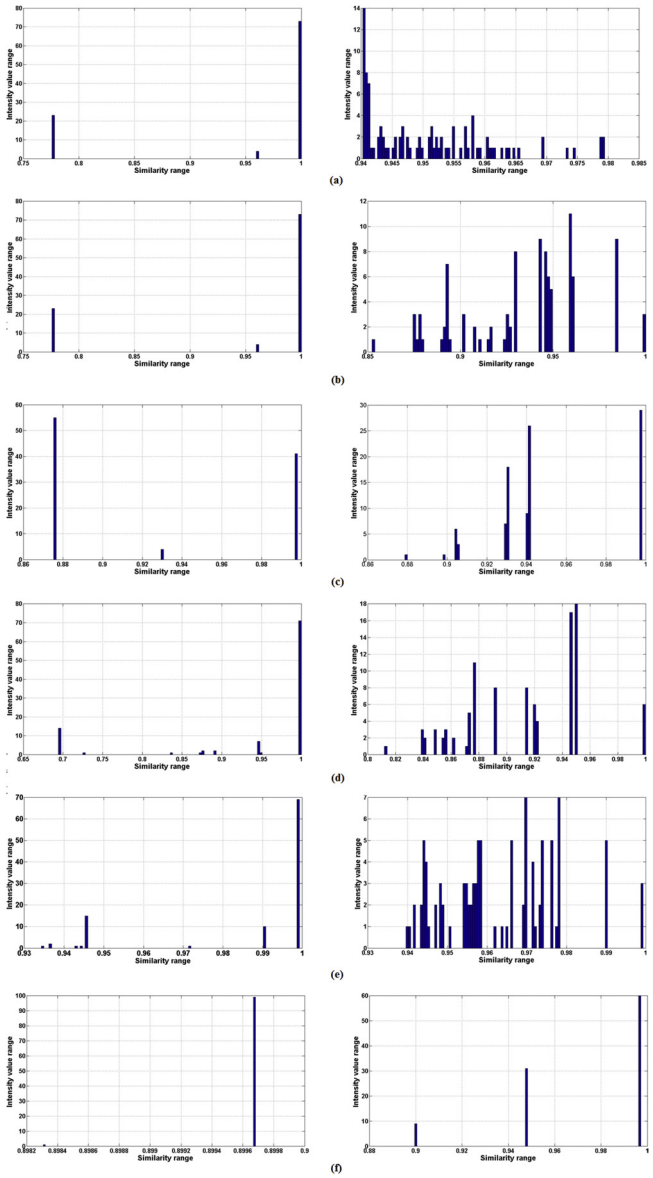

Fig. 12. Solution quality distributions of 100 repeated experiments conducted via ABC (left) and RS (right) respectively in: (a) Case 1; (b) Case 2; (c) Case 3; (d) Case 4; (e) Case 5; and (f) Case 6.

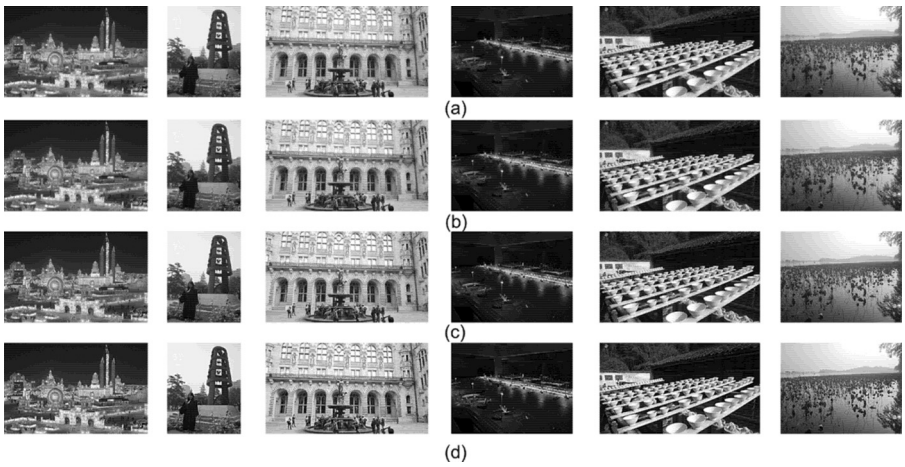

Fig. 13. On the performance of lateral inhibition in test image enhancement: (a) $\rho = 2$;; (b) $\rho = 3$; (c) $\rho = 10$; and (d) $\rho = 20$.

set as $SN/2 = 20$ and Limit = 50 · Dim · SN, wherein Dim = 2 denoted the optimization problem dimensionality. Experiments were carried out on six cases, as depicted in Fig. 4.

In the first round of experiments, we investigate whether it is necessary to adopt evolutionary algorithms in searching for the best-match location for image retrieval. ABC algorithm, full searcher (FS), and random searcher (RS) were respectively adopted for solving each of the aforementioned six schemes. Specifically, the complete time was recorded for each search algorithm, and each single type of experiment was repeated for 100 times. Comparative results are shown in Fig. 5.

The second round of experiments further investigates the advantage of the leading algorithm (among ABC, FS, and RS) over its competitors in each of the six cases. Let us take Case 1 for example: image retrieval problem was solved again using each of the three searchers, but the searching process should be terminated by 6.98 s, even if the best-match location is not yet found. Each single type of experiment was repeated for 100 times, and those 100 results are plotted simultaneously in one figure for each case using either ABC or FS, as depicted in Figs. 6–11. To show the search quality more clearly, distributions of the 100 results in each single type of experiment are illustrated in Fig. 12.

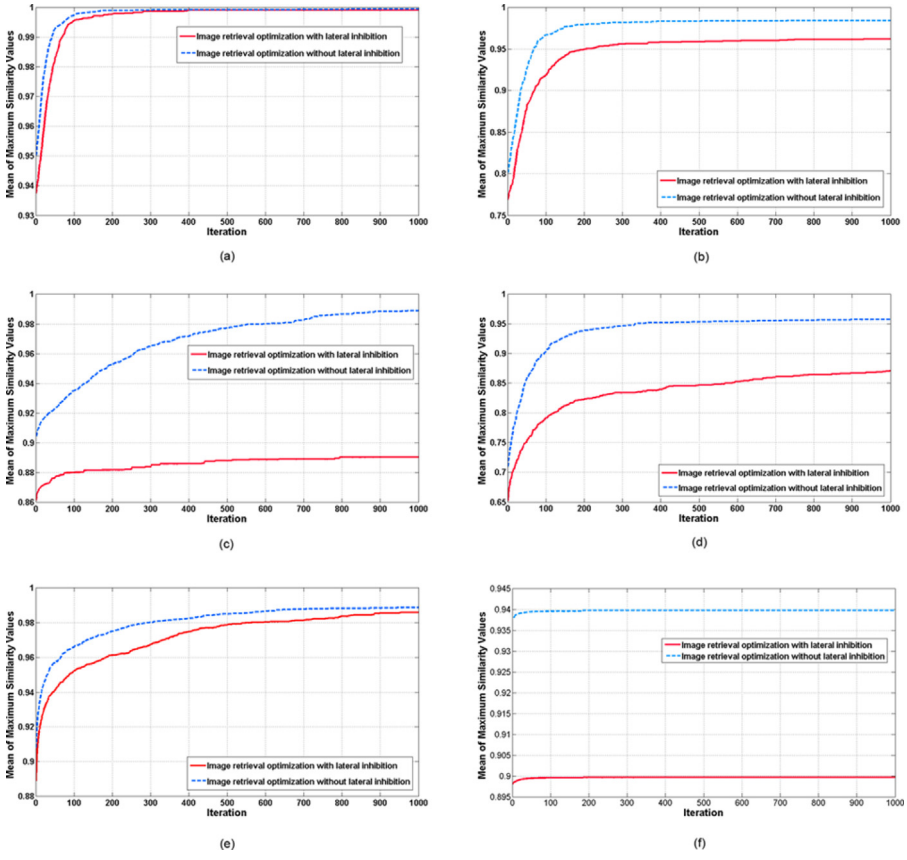

Fig. 14. On the performance of lateral inhibition in facilitating image retrieval: (a) Case 1; (b) Case 2; (c) Case 3; (d) Case 4; (e) Case 5; and (f) Case 6.

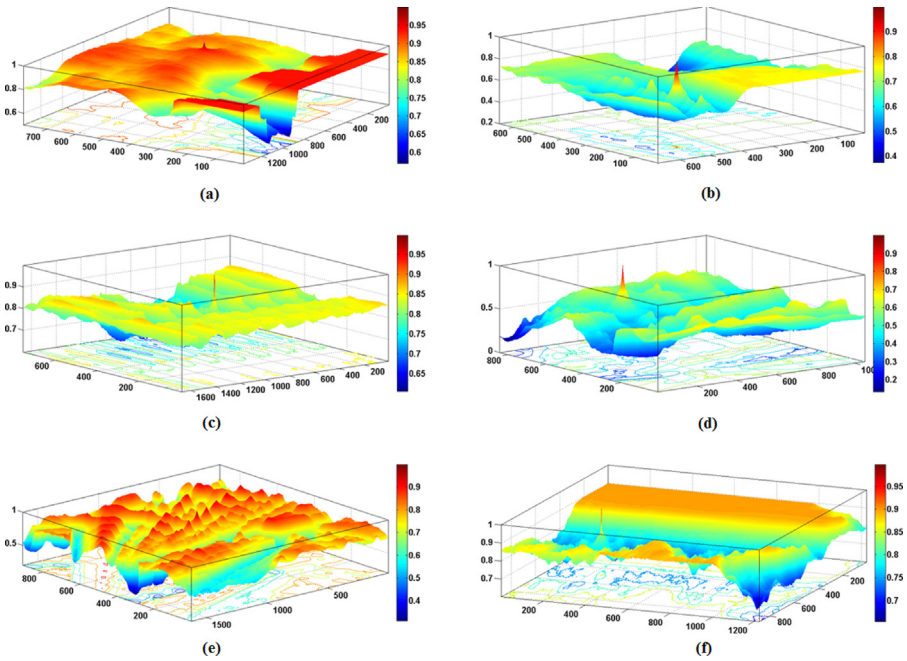

Fig. 15. Solution space in the converted 2-dimensional optimization problem: (a) for Case 1; (b) for Case 2; (c) for Case 3; (d) for Case 4; (e) for Case 5; and (f) for Case 6.

The third round of experiments concerns how the inhibition weight matrix would influence image enhancement performance. In addition to the default definition in Fig. 2, inhibition weight matrixes with more rings were considered. Simulations based on those six test images and various inhibition weight matrixes are reported in Fig. 13.

At last, the fourth round of experiments concerns how lateral inhibition facilitates the searching process in image retrieval when ABC algorithm is adopted. Experimental results are summarized in Fig. 14.

4. Discussions

Given that image retrieval is considered as a 2-dimensional optimization problem, whether evolutionary algorithms are advantageous over random searching and full searching methodologies deserves investigation. Unfortunately, this fundamental issue has been disregarded in nearly all of the previous publications [5]. According to the experimental results in the first round (Fig. 5), one obtains that ABC (on behalf of evolutionary algorithms) saves time to find the best-match location in Cases 1–5 but significantly lags in Case 6. This indicates that the search advantage in using evolutionary algorithms is not as solid as expected in Refs. [19–24]. In spite of the defects in using evolutionary algorithms, their potentials may contribute to fast perception in autonomous driving [45–48]. To investigate the performance of ABC even further, solution space in each case is illustrated in Fig. 15. According to the surface shapes, all the six cases are classified into three groups: (i) a “horn” on a flat space, (ii) a “pinpoint” on a flat space, and (iii) a “hilly” space. Cases 1, 2, and 4 fall into category (i), Cases 3 and 6 are in category (ii), and Case 5 is in category (iii). When handling the three cases in category (i), ABC has obvious advantages over RS and FS, as depicted in Fig. 5. In contrast, ABC becomes not so efficacious in dealing with cases in category (ii). The additional difficulties for ABC to handle either case in category (ii) originate from the sharp pinpoint. Specifically, the pinpoint in the solution space denotes the global optimum. A sharp pinpoint indicates that ABC is difficult to converge to optimum from surrounding locations in the solution space. On the other hand, gradients around the optimum are relatively low in cases of category (i), thus convergence is achieved with ease. Regarding category (iii), i.e., Case 5, ABC is capable of finding the global optimum, without getting attracted by multiple local optimums. The solution space of Case 5 is distinct from the remaining five ones because there are multiple similar objects in the test image (see Fig. 4(i)).

The second round of experiments concerns the gaps among the three searchers. As FS is the only algorithm among all the three that guarantees finding global optimum, we made comparisons between ABC and RS only. Viewing the results shown in Figs. 6–11 together with the distributions depicted in Fig. 12, one may notice that ABC tends to converge at fewer kinds of solutions than RS by certain computation time. That is because the crossover & mutation operations in ABC help making evolutions efficiently when gradient-based information is available to direct the optimum. Conversely regarding RS, the searching behavior from 0.99 to 1 is the same as the searching behavior from any other one (e.g., from 0.80 to 0.81). The randomness in RS renders the solution distribution in repeated experiments.

The third round of experiments confirms that the image enhancement performance becomes evident as ρ increases. Thus lateral inhibition is efficient as a preprocessing step. Following this, the fourth round of experiments concerns whether this preprocessing step really works to facilitate the numerical optimization process. Unfortunately, there is none appreciable evidence that indicates the facilitation, according to the comparative evolutionary curves shown in Fig. 14.

5. Conclusions

In this work, original image retrieval schemes are transformed into 2-dimensional optimization problems and then solved by ABC algorithm. Investigations have been made on several fundamental issues in this research topic. Contributions of this paper lie in the following few points.

First, we have investigated whether evolutionary algorithms are advantageous over full searcher and random searcher. The conclusion is that advantages of ABC are not solid. In handling intricate image retrieval problems, evolutionary algorithms may perform no

better than random searcher or full searcher. This is because evolutionary algorithms facilitate the convergence via gradient-based information, which is difficult to obtain in intricate cases.

Second, we have investigated whether the prevailing preprocessing step, namely, lateral inhibition contributes to easing the image retrieval optimization. Unfortunately, all of our preliminary simulations indicate that lateral inhibition provided no help at all. This conclusion has directly wiped out most of the contributions presented in Refs. [19–24]. This phenomenon may be taken as a good lesson: never take for granted in following previous studies without solid supporting theories and/or experiments.

Acknowledgments

The author thanks Dr. Y. Li, Mr. H. Sun, Dr. R. Chiong, and Prof. R. Zhang for their suggestions and support. This work is sponsored by the 6th National College Students' Innovation & Entrepreneurial Training Program of China under Grant 201210006050. Complete source codes of this work are available at http://www.mathworks.com/matlabcentral/fileexchange/55994.

Appendix.

Proof of Lemma 2. Suppose that $\mathbf{X}_1$ and $\mathbf{X}_2$ are two arbitrarily selected solutions in $\mathbf{D}$, such that $fun(\mathbf{X}_1) < fun(\mathbf{X}_2)$. Given that $fun(\bullet)$ is uniformly continuous, for $\varepsilon_0 = (fun(\mathbf{X}_2) - fun(\mathbf{X}_1)/2) > 0$, $\delta_1 > 0$ exists, such that $|fun(\mathbf{X}_1) - fun(\mathbf{X})| < \varepsilon_0$ for any $\mathbf{X} \in U(\mathbf{X}_1, \delta_1)$. Herein, $U(\mathbf{X}_1, \delta_1)$ denotes $\{\mathbf{Y} | \|\mathbf{Y} - \mathbf{X}_1\| < \delta_1\}$, where $\|\cdot\|$ refers to the Euclidean norm on $\mathbb{R}^n$. Moreover, for ε_0, $\delta_2 > 0$ exists, such that $|fun(\mathbf{X}_1) - fun(\mathbf{X})| < \varepsilon_0$ holds true regardless of any $\mathbf{X} \in U(\mathbf{X}_2, \delta_2)$.

By defining $\delta^* = \min\{\delta_1, \delta_2\}$, the following can be obtained:

$$fun(\mathbf{X}_1) - \varepsilon_0 < fun(\mathbf{X}) < fun(\mathbf{X}_1) + \varepsilon_0, \quad \forall \mathbf{X} \in U(\mathbf{X}_1, \delta*), \tag{A1}$$

$$fun(\mathbf{X}_2) - \varepsilon_0 < fun(\mathbf{X}) < fun(\mathbf{X}_2) + \varepsilon_0, \quad \forall \mathbf{X} \in U(\mathbf{X}_2, \delta*). \tag{A2}$$

$fun(\bullet)$ is uniformly continuous. Thus, if we integrate $fun(\mathbf{X})$ on $U(\mathbf{X}_1, \delta^*)$ and $U(\mathbf{X}_2, \delta^*)$, then we obtain $IS_1 = \oint_{U(\mathbf{X}_1, \delta*)} fun(\mathbf{X}) d\mathbf{X}$ and $IS_1 = \oint_{U(\mathbf{X}_2, \delta*)} fun(\mathbf{X}) d\mathbf{X}$, which satisfy the following:

$$\begin{aligned} IS_1 &< \oint_{U(\mathbf{X}_1, \delta*)} (fun(\mathbf{X}_1) + \varepsilon_0) d\mathbf{X} \\ &= \frac{fun(\mathbf{X}_1) + fun(\mathbf{X}_2)}{2} \cdot \oint_{U(\mathbf{X}_1, \delta*)} d\mathbf{X}, \end{aligned} \tag{A3}$$

$$\begin{aligned} IS_2 &> \oint_{U(\mathbf{X}_2, \delta*)} (fun(\mathbf{X}_1) - \varepsilon_0) d\mathbf{X} \\ &= \frac{fun(\mathbf{X}_1) + fun(\mathbf{X}_2)}{2} \cdot \oint_{U(\mathbf{X}_2, \delta*)} d\mathbf{X}, \end{aligned} \tag{A4}$$

Obviously, $\oint_{U(\mathbf{X}_1, \delta*)} d\mathbf{X} = \oint_{U(\mathbf{X}_2, \delta*)} d\mathbf{X}$. Thus, Eqs. (A3) and (A4) render $IS_1 < IS_2$.

If N_f (finite) arbitrarily selected feasible solutions satisfy $fun(\mathbf{X}_1) \le fun(\mathbf{X}_2) \le \ldots \le fun(\mathbf{X}_{N_f})$, then $\forall i, j \in 1, 2, \ldots, N_f$, $i < j$ $\exists \delta^* = \delta_{ij} > 0$ such that $IS_i \le IS_j$. In this case, if we select

$$\delta* = \min\{\delta_{ij} | \forall i, j \in 1, 2, \ldots, N_f, \quad i \ne j\}, \tag{A5}$$

then $IS_1 \le IS_2 \le \ldots \le IS_{N_f}$ hold true constantly.

Let us consider adding arbitrarily selected feasible solutions $\mathbf{X}_i$ to an originally empty set $\{\emptyset\}$ one at a time. Lemma 1 states that $\delta_0 > 0$ always exists, such that $\mathbf{D} \subseteq \bigcup_{i=1}^{N'_f} U(\mathbf{X}_i, \delta_0)$ as N'_f is increased by one at a time. Such (arbitrarily selected) feasible solutions are added to this set until $\delta_0 \ge \delta^*$ exists such that $\forall i, j = 1, 2, \ldots, N'_f$, if $fun(\mathbf{X}_i) \le fun(\mathbf{X}_j)$, then $IS_i \le IS_j$. Herein, δ^* is defined in Eq. (A5). Thus, infinite feasible solutions in the domain $\mathbf{D}$ can be expressed by a finite number of open covers $\{U(\mathbf{X}_i, \delta_0), i = 1, 2, \ldots, N'_f\}$ because one can always find a finite number of elements that completely reflect the inequality relationship between the qualities of any two specified candidate solutions. That is, the pursuit for $\underset{\mathbf{X}^{opt}}{arg}(fun(\mathbf{X}^{opt}) = \max\{fun(\mathbf{X}) | \forall \mathbf{X} \in \mathbf{D}\})$ can be transformed into the pursuit for $\underset{U(\mathbf{X}^{opt}, \delta_0)}{arg}\left(\oint_{U(\mathbf{X}^{opt}, \delta_0)} fun(\mathbf{X}) d\mathbf{X} = \max\{IS_i | i = 1, 2, \ldots, N'_f\}\right)$ on the condition that $fun(\bullet)$ is uniformly continuous on $\mathbf{D}$.

Proof of Lemma 3. In ABC algorithm, the greedy selection is the sole cause of the transition of the current-best solutions. Each transition probability is in the range of $0 \le tp_{ij} \le 1$. For each $\mathbf{S}_i$ at step t, the transition possibilities to every $\mathbf{S}_j$ at step $(t+1)$ can be summed up to form a certain event, i.e.,

$$\sum_{j=1}^{M} tp_{ij} = 1, \ (\forall i \in 1, 2, \ldots, M). \tag{A6}$$

Therefore, $\mathbf{TP}$ is a stochastic matrix. The transition procedure of current-best solutions between any two steps is a stochastic process.

Proof of Lemma 4. Given that the size of $\mathbf{S}$ is finite, the Markov process is also finite. In addition, according to the definition of greedy selection, the current-best solution at step $(t+1)$ should be not worse than that at step t for $\forall t > 0$. In other words, the current-best solution at step $(t+1)$ depends only on the current-best solution at step t. Moreover, the step index t (which refers to the cycle of iteration variable *iter* in ABC algorithm) does not exist in any relevant equation. That is, the step index t does not have any effect on the transition of current-best solutions. Considering the three aforementioned aspects, we confirm that the transition of current-best solution in ABC algorithm is a finite homogeneous Markov process.

Proof of Lemma 5. The entry in the ith row and jth column of a new matrix $(\mathbf{TP}_{t,t+1} \cdot \mathbf{TP}_{t+1,t+2})_{N_{fs} \times N_{fs}}$ should be $\sum_{m=1}^{N_{fs}} tp_{im}^{t} \cdot tp_{mj}^{t+1}$. According to the independence between step t and $t+1$ as confirmed in Lemma 4, $tp_{im}^{t} \cdot tp_{mj}^{t+1}$ denotes the transition probability of current-best solution from $\mathbf{S}_i$ to $\mathbf{S}_m$ and then to $\mathbf{S}_j$. In other words, $\sum_{m=1}^{N_{fs}} tp_{im}^{t} \cdot tp_{mj}^{t+1}$ represents the probability of a one-step transition from $\mathbf{S}_i$ to $\mathbf{S}_j$. Therefore, the transition probability $\sum_{m=1}^{N_{fs}} tp_{im}^{t} \cdot tp_{mj}^{t+1}$ is equal to the entry in the ith row and jth column of $\mathbf{TP}_{t,t+2}$. This conclusion holds for any integer index $i, j \in [1, N_{fs}]$. This phenomenon indicates that $\mathbf{TP}_{t,t+1} \cdot \mathbf{TP}_{t+1,t+2} = \mathbf{TP}_{t,t+2}$ for any $t > 0$.

Proof of the Theorem. The greedy selection strategy implies that $tp_{mn} = 0$ for any m, n, that satisfies $IS_m \ge IS_n$ [49]. This relationship, together with Eq. (A6), yields

$$\mathbf{TP}_{t,t+1} = \begin{pmatrix} 1 & 0 & \cdots & 0 \\ tp_{21}^{t} & tp_{22}^{t} & \cdots & 0 \\ \vdots & \vdots & \ddots & \vdots \\ tp_{N_{fs}1}^{t} & tp_{N_{fs}2}^{t} & \cdots & tp_{N_{fs}N_{fs}}^{t} \end{pmatrix}_{N_{fs} \times N_{fs}}. \tag{A7}$$

The matrix $\mathbf{TP}_{t,t+1}$ is reducible as it can be expressed in a low triangular matrix form $\begin{pmatrix} 1 & 0 \\ \mathbf{R} & \mathbf{T} \end{pmatrix}$, where

$$\mathbf{R} = \begin{bmatrix} tp_{21} \\ tp_{31} \\ \vdots \\ tp_{M1} \end{bmatrix}_{(M-1)\times 1}, \quad \mathbf{T} = \begin{bmatrix} tp_{22} & \cdots & 0 \\ \vdots & \ddots & \vdots \\ tp_{M2} & \cdots & tp_{MM} \end{bmatrix}_{(M-1)\times(M-1)}$$

In addition, Lemma 4 indicates that the process involves a finite homogeneous Markov process. Thus, by applying Lemma 5 and Eq. (7), the following can be obtained:

$$\lim_{k\to\infty} \mathbf{TP}_{1,k} = \lim_{k\to\infty} \left(\prod_{i=1}^{k-1} \mathbf{TP}_{1,2} \right) \tag{A8}$$

Then, Lemma 6 and Eq. (A8) obtain

$$\lim_{k\to\infty} \left(\prod_{i=1}^{k-1} \mathbf{TP}_{1,2} \right) = \begin{pmatrix} 1 & 0 \\ \mathbf{R}_\infty & 0 \end{pmatrix} = \lim_{t\to\infty} \mathbf{TP}_{1,t}. \tag{A9}$$

$\lim_{t\to\infty} \mathbf{TP}_{1,t}$ denotes the matrix of current-best solution transition probabilities from the initial step to an infinite step.

Given that $\lim_{t\to\infty} \mathbf{TP}_{1,t}$ is also a stochastic matrix, each row of $\lim_{t\to\infty} \mathbf{TP}_{1,t}$ can be summed up to 1. That is,

$$\mathbf{R}_\infty = \begin{bmatrix} tp_{21} \\ \vdots \\ tp_{N1} \end{bmatrix} = \begin{bmatrix} 1 \\ \vdots \\ 1 \end{bmatrix}, \tag{A10}$$

thereby indicating that any initial current-best solution will eventually converge into the global optimum with 100% probability at a sufficiently large step.

References

[1] O. Regniers, J. Costa, G. Grenier, C. Germain, L. Bombrun, Texture based image retrieval and classification of very high resolution maritime pine forest images, in: Proc 2013 IEEE International Geoscience and Remote Sensing Symposium, IEEE, 2013, pp. 4038–4041.

[2] J. Yang, J. Liu, Q. Dai, An improved Bag-of-Words framework for remote sensing image retrieval in large-scale image databases, Int. J. Digit. Earth 8 (4) (2015) 273–292.

[3] J. Pisek, M. Lang, J. Kuusk, A note on suitable viewing configuration for retrieval of forest understory reflectance from multi-angle remote sensing data, Remote Sens. Environ. 156 (2015) 242–246.

[4] B. Demir, L. Bruzzone, A novel active learning method in relevance feedback for content-based remote sensing image retrieval, IEEE Trans. Geosci. Remote Sens. 53 (5) (2015) 2323–2334.

[5] B. Li, Li. Gong, Y. Li, A novel artificial bee colony algorithm based on internal-feedback strategy for image template matching, Sci. World J. 2014 (906861) (2014) 1–14, http://dx.doi.org/10.1155/2014/906861.

[6] F. Zhang, Y. Song, W. Cai, A. Hauptmann, S. Liu, S. Pujol, R. Kikinis, M. Fulham, D. Feng, M. Chen, Dictionary pruning with visual word significance for medical image retrieval, Neurocomputing 177 (12) (2015) 75–88.

[7] A. Kumara, S. Dyerb, J. Kima, C. Lia, P. Leongb, M. Fulhama, D. Fenga, Adapting content-based image retrieval techniques for the semantic annotation of medical images, Comput. Med. Imaging Graph. 49 (2016) 37–45.

[8] J. Kalpathy-Cramer, A. Herrera, D. Demner-Fushman, S. Antani, S. Bedrick, H. Müller, Evaluating performance of biomedical image retrieval systems – an overview of the medical image retrieval task at ImageCLEF 2004–2013, Comput. Med. Imaging Graph. 39 (2015) 55–61.

[9] K. Trojacanec, I. Kitanovski, I. Dimitrovski, S. Loshkovska, Medical image retrieval for Alzheimer's disease using data from multiple time points, in: Proc. ICT Innovations 2015, Springer International Publishing, 2016, pp. 215–224.

[10] H. Qi, W. Snyder, Content-based image retrieval in picture archiving and communications systems, J. Digit. Imaging 12 (1) (1999) 81–83.

[11] T. Lehmann, M. Guld, C. Thies, B. Fischer, D. Keysers, M. Kohnen, H. Schubert, B. Wein, Content-based image retrieval in medical applications for picture archiving and communication systems, Med. Imaging 2003 (2003) 109–117, International Society for Optics and Photonics.

[12] X. Liao, P. Chitrakar, C. Zhang, G. Warner, Object-of-interest retrieval in social media image databases for e-Crime forum detection, Int. J. Multimed. Data Eng. Manag. 6 (3) (2015) 32–50.

[13] K. Shriram, P. Priyadarsini, A. Baskar, An intelligent system of content-based image retrieval for crime investigation, Int. J. Adv. Intell. Paradig. 7 (3) (2015) 264–279.

[14] L. An, C. Zou, L. Zhang, B. Denney, Scalable attribute-driven face image retrieval, Neurocomputing 172 (2016) 215–224.

[15] B. Ionescu, A. Popescu, A. Radu, H. Müller, Result diversification in social image retrieval: a benchmarking framework, Multimed. Tools Appl. 75 (2) (2016) 1301–1331.

[16] Q. Liu, Z. Li, Projective nonnegative matrix factorization for social image retrieval, Neurocomputing 172 (2016) 19–26.

[17] Y. Rui, T. Huang, S. Chang, Image retrieval: current techniques, promising directions, and open issues, J. Vis. Commun. Image Represent. 10 (1) (1999) 39–62.

[18] Y. Liu, D. Zhang, G. Lu, W. Ma, A survey of content-based image retrieval with high-level semantics, Pattern Recognit. 40 (1) (2007) 262–282.

[19] F. Liu, H. Duan, Y. Deng, A chaotic quantum-behaved particle swarm optimization based on lateral inhibition for image matching, Optik 123 (21) (2012) 1955–1960.

[20] X. Wang, H. Duan, D. Luo, Cauchy biogeography-based optimization based on lateral inhibition for image matching, Optik 124 (22) (2013) 5447–5453.

[21] L. Gan, H. Duan, Biological image processing via Chaotic Differential Search and lateral inhibition, Optik 125 (9) (2014) 2070–2075.

[22] Z. Zhang, H. Duan, A hybrid particle chemical reaction optimization for biological image matching based on lateral inhibition, Optik 125 (19) (2014) 5757–5763.

[23] C. Zhang, H. Duan, Biological lateral inhibition and electimize approach to template matching, Optik 126 (7) (2015) 769–773.

[24] L. Huang, H. Duan, Y. Wang, Hybrid bio-inspired lateral inhibition and imperialist competitive algorithm for complicated image matching, Optik 125 (1) (2014) 414–418.

[25] B. Li, Z. Shao, Precise trajectory optimization for articulated wheeled vehicles in cluttered environments, Adv. Eng. Softw. 92 (2016) 40–47.

[26] B. Li, M. Lin, Q. Liu, Y. Li, C. Zhou, Protein folding optimization based on 3D off-lattice model via an improved artificial bee colony algorithm, J. Mol. Model. 21 (10) (2015) 1–15.

[27] B. Li, Y. Li, H. Cao, H. Salimi, Image enhancement via lateral inhibition: an analysis under illumination changes, Optik 127 (12) (2016) 5078–5083.

[28] G. Zhu, S. Kwong, Gbest-guided artificial bee colony algorithm for numerical function optimization, Appl. Math. Comput. 217 (7) (2010) 3166–3173.

[29] I. Aydoğdu, A. Akın, M. Saka, Design optimization of real world steel space frames using artificial bee colony algorithm with Levy flight distribution, Adv. Eng. Softw. 92 (2016) 1–14.

[30] B. Li, Y. Li, L. Gong, Protein secondary structure optimization using an improved artificial bee colony algorithm based on AB off-lattice model, Eng. Appl. Artif. Intell. 27 (2014) 70–79.

[31] W. Gao, S. Liu, L. Huang, A global best artificial bee colony algorithm for global optimization, J. Comput. Appl. Math. 236 (11) (2012) 2741–2753.

[32] B. Li, Research on WNN modeling for gold price forecasting based on improved artificial bee colony algorithm, Comput. Intell. Neurosci. 2014 (270658) (2014) 1–10, http://dx.doi.org/10.1155/2014/270658.

[33] F. Kang, J. Li, Z. Ma, Rosenbrock artificial bee colony algorithm for accurate global optimization of numerical functions, Inf. Sci. 181 (16) (2011) 3508–3531.

[34] B. Li, R. Chiong, M. Lin, A balance-evolution artificial bee colony algorithm for protein structure optimization based on a three-dimensional AB off-lattice model, Comput. Biol. Chem. 54 (2015) 1–12.

[35] W. Xiang, M. An, An efficient and robust artificial bee colony algorithm for numerical optimization, Comput. Oper. Res. 40 (5) (2013) 1256–1265.

[36] M. Kiran, H. Hakli, M. Gunduz, H. Uguz, Artificial bee colony algorithm with variable search strategy for continuous optimization, Inf. Sci. 300 (2015) 140–157.

[37] I. Babaoglu, Artificial bee colony algorithm with distribution-based update rule, Appl. Soft Comput. 34 (2015) 851–861.

[38] B. Li, Y. Yao, An edge-based optimization method for shape recognition using atomic potential function, Eng. Appl. Artif. Intell. 35 (2014) 14–25.

[39] P. Loubière, A. Jourdan, P. Siarry, R. Chelouah, A sensitivity analysis method for driving the Artificial Bee Colony algorithm's search process, Appl. Soft Comput. 41 (2016) 515–531.

[40] B. Li, H. Cao, M. Hu, C. Zhou, Shape matching optimization via atomic potential function and artificial bee colony algorithms with various search strategies, in: Proc. of 8th International Symposium on Computational Intelligence and Design, December, IEEE, 2015, pp. 1–4.

[41] E. Borel, Leçons sur la théorie des fonctions, Gauthier-Villars et fils, 1898.

[42] A. Eiben, E. Aarts, K. Van, Global Convergence of Genetic Algorithms: A Markov Chain Analysis. In Parallel Problem Solving from Nature, Springer Berlin Heidelberg, 1991, pp. 3–12.

[43] E. Seneta, E. Seneta, Non-Negative Matrices: An Introduction to Theory and Applications, Wiley, New York, 1973, pp. 52–54.

[44] M. Iosifescu, Finite Markov Processes and Their Applications, Wiley, Chichester, 1980.

[45] B. Li, Z. Shao, A unified motion planning method for parking an autonomous vehicle in the presence of irregularly placed obstacles, Knowl.-Based Syst. 86 (2015) 11–20.

[46] B. Li, et al., Time-optimal maneuver planning in automatic parallel parking using a simultaneous dynamic optimization approach, IEEE Trans. Intell. Transp. Syst. (2016) (in press).
[47] B. Li, Z. Shao, An incremental strategy for tractor-trailer vehicle global trajectory optimization in the presence of obstacles, in: Proc. 2015 IEEE International Conference on Robotics and Biomimetics, IEEE, 2015, pp. 1447–1452.
[48] B. Li, Z. Shao, Time-optimal trajectory planning for tractor-trailer vehicles via simultaneous dynamic optimization, in: Proc. 2015 IEEE/RSJ International Conference on Intelligent Robots and Systems, IEEE, 2015, pp. 3844–3849.
[49] G. Rudolph, Convergence analysis of canonical genetic algorithms, IEEE Trans. Neural Netw. 5 (1) (1994) 96–101.